International Journal of Environmental Sciences
ISSN: 2229-7359
Vol. 11 No. 1s, 2025
https://www.theaspd.com/ijes.php

The Effect of Polar Solutions on the Nanoparticles ZnO Characterization: Experimental Study for Photodegradation of Phenol from Wastewater

Sara Basheer Mohamed[1*], Khaleel I. Hamad[2], Hayder Al-Naseri[3] and Nalan Turkoz Karakulluukcu[4]

[1,2,3] College of Engineering, Tikrit University, Chemical Engineering Department, Ministry of Higher Education and Scientific Research

[4] Karadeniz Advanced Technology Research and Application Center , Ondokuz Mayis University , Atakum ,55200 Samsun , Turkiye

[1]Email:sara.b.mohameed42154@st.tu.edu.iq

[2]Email:khalil.edan@tu.edu.iq

[3]Email:h.alnasri@tu.edu.iq

[4]Email:nturkoz@omu.edu.tr

ABSTRACT: *This study explores phenol removal from industrial wastewater using a UV slurry bubble column reactor with pre-synthesized ZnO nanoparticles. ZnO was prepared via the sol-gel method using three solvents deionized water (CAT-1), ethanol (CAT-2), and glycerol (CAT-3). Zinc oxide nanoparticles were synthesized through the sol-gel method prior to their use in the photocatalytic process. Glycerol led to smaller particles with higher surface area due to its high viscosity and ability to control nucleation. These ZnO particles were then used in a UV slurry bubble column reactor, where UV light excited the ZnO, producing electron-hole pairs. These pairs interacted with water and oxygen to create hydroxyl and superoxide radicals. These radicals attacked phenol molecules, breaking them down into intermediates and finally into CO_2 and H_2O. This degradation followed pseudo-first-order kinetics, and the best performance was recorded with the glycerol-derived ZnO (CAT-3), confirming its suitability for wastewater treatment. CAT-3 calcined at 400°C showed the best surface area and crystallinity. The photocatalytic process achieved over 90% phenol degradation under optimal conditions. ZnO acts as a semiconductor, where UV light excites electrons, generating reactive species that oxidize phenol into harmless by-products. This method provides an efficient, eco-friendly approach to treating industrial wastewater.*

Keywords: *ZnO nanoparticles; Sol-gel method; Polar solvents; Photocatalytic degradation; Phenol removal; Wastewater treatment.*

1 INTRODUCTION

Phenol is regarded as a major environmental contaminant and may lead to water pollution. Its existence in water comes from two sources, either as a natural occurrence or through anthropogenic activities and it was classified as an organic compound and can be determined by a hydroxyl (OH) group(s) attached to one or more of its aromatic rings [1]. There are different techniques have been utilized to reduce and remove the phenol from the aqueous solution physical treatment (distillation, adsorption, and extraction), and chemical treatment (chemical oxidation, biodegradation, electrochemical oxidation). Advanced oxidation processes (AOPs) have shown promise in the destruction or mineralization of many organic pollutants in water and wastewater treatment. These processes generate highly reactive hydroxyl radicals (HO·) [2]. Photocatalytic processes have been often used and studied in recent years and they are described as an effective type of AOP to treat and degrade organic pollutants. The generation of radicals takes place on the surface of the catalyst. The photocatalytic process enables the activation of a semiconductor particle (SMP) material via radiation at a specific wavelength (λ), heat, or external oxidants [3].

Recently, the synthesis of nanoscale materials has garnered attention due to their distinctive mechanical, physical, optical, and magnetic properties. The characteristics of nanoparticles encourage a wide range of applications in diverse technological domains, including ceramics, structural

components, magnetic data storage, energy storage, electronics, and catalysis[4]. Nanoparticle applications in the size range of 1 to 100 nm have garnered significant attention in recent years due to their novel characteristics and have been the topic of much study [5].

Zinc oxide (ZnO) has been intensively studied because of its high photosensitivity, nontoxic nature, large bandgap ($3.3\ eV$), and low cost [6]. Thereby,ZnO is widely used as an efficient and inexpensive semiconductor photocatalyst for the decomposition of most organic chemicals and energy applications [7][6], in the field of materials science is categorized as a semiconductor in group II-VI. Its covalence is at the interface between ionic and covalent semiconductors [8][7] and can be obtained in the form of a hexagonal wurtzite crystalline structure and are intriguing to investigate due to their distinctive physical properties, as well as their wide range of morphologies and their enticing electrical and optical properties [9][10][11]

The particle size of ZnO in these powders is a crucial determinant for the specific application [12]. ZnO is a promising option due to its unique chemical, surface, and nanostructured characteristics, particularly for gas sensing and catalysis applications where the particles' surface area must be exposed to the target gas [13]. In various literature, it is evident that nano ZnO exhibits superior performance in comparison to bulk ZnO [14].

In recent years researchers have focused more on the synthesis and properties of ZnO nanoparticles due to their application in advanced technologies [12]. Nowadays, several techniques are employed to synthesize ZnO nanoparticles, including sol-gel synthesis, hydrothermal/solvo thermal methods, microemulsion methods, precipitation, and physical vapor deposition. Chemical synthesis is a crucial method that involves the use of several precursors and certain variables such as temperature, time, and reactant concentration [15]. The main advantage of chemical methods is their ability to produce particles with specific dimensions, composition, and structure. These particles can find application in a variety of fields, including sensing, catalysis, and electrical devices. Furthermore, the synthesis carried out by some chemical processes, specifically the sol-gel approach, requires lower processing temperatures and less energy, making it more cost-effective than physical procedures [16]. The synthesis of solid catalysts using the sol-gel method has been reported by several research teams since the 1980s[17]. The sol-gel process involves the transition of a system from a liquid "sol" into a solid "gel" phase, enabling precise control over the chemical composition and uniformity of the resulting nanoparticles. This method also allows for low-temperature processing and scalability, making it an efficient approach for synthesizing ZnO nanoparticles.

However, the nanoparticle structures have been controlled via different parameters, for instance, pH, solvent, raw material, precursors, and method of synthesis[18]. Therefore, numerous investigations have been conducted to address the effect of these parameters. Among these parameters, the solvent type where significantly affects the structure of the nanoparticle[19], [20].ZnO nanoparticles are specified by high surface energy and large specific surface area. Thereby, nanoparticles try to agglomerate easily during the preparation. Therefore, most methods need a low concentration of precursors and utilize a large amount of stabilizers (i.e., water or organic solvent)[8], [21], [22]. Additionally, using water in synthesis processes frequently results in hard agglomerates, which hinders the utilization of ZnO nanoparticles[23]. The polyol method was demonstrated to be effective for synthesizing metal oxide nanoparticles[24]. ZnO nanoparticles have been effectively produced in diverse polyol media, including 1,4-butanediol, ethylene glycol, diethylene glycol, tetraethylene glycol, and 1,3-propanediol[20], [25]–[27].

[28] suggested three different solvents distilled water, absolute ethanol, and isopropanol to synthesis the ZnO from the zinc acetate. There results exhibit that using distilled water, absolute ethanol, and isopropanol created nanoparticles with ellipse, rod, and spherical shapes, respectively.Meanwhile, solvent of isopropanol creates more homogenous size and shape of ZnO. [29]used NaOH and KOH in aqueous solution with Zinc Nitrate as precursor to create ZnO nanoparticles via sol-gel process. The data obtained illustrated that the aqueous solution significantly

affected the surface morphology, optical properties, and structural integrity of ZnO. Practically, the particle size decreased due to using the KOH. [30] investigated the effects of precursors and solutions on the nanoparticle's properties of the ZnO, where utilized (oxalic acid, zinc oxalate, and zinc acetate) as precursors, and three different solvents (water, ethanol, propanol). This investigation reported that the average diameter of the nanoparticles measured was 79.55 nm, 83.86 nm, and 85.59 nm using ethanol, propanol, and water, respectively. When compared to other solvents under research, ZnO particles displayed a higher degree of crystallization in water. [19]prepared ZnO nanoparticles from aqueous solutions of zinc chloride ($ZnCl_2$) and hydroxide at room temperature using a glycerol stabilizer. Concentrated zinc was obtained from $ZnCl_2$ aqueous solutions that were as high as 65–80 wt%. The molar ratio of glycerol to Zn^{2+} and the concentration of $ZnCl_2$ solutions clearly affected the sizes and forms of the ZnO nanoparticles. With increasing $ZnCl_2$ solution content and glycerol to Zn^{2+} mole ratio, the shape of ZnO nanoparticles changed from rods about 50–120 nm long and 30–70 nm in diameter to globular with diameters of about 20 nm.

Based on mentioned, we explore the synthesis of ZnO nanoparticles using the sol-gel method, focusing on the optimization of parameters to achieve desired structural and functional properties, this technique is an economical and efficient method for producing uniform, highly pure, and high-quality nano powders. It is well recognized as a traditional and industrial approach for synthesizing nanoparticles with varying chemical compositions [31][32]. The main objective of this study is the synthesis of ZnO nanoparticles by the sol-gel method and to studytheir characterization. The sol-gel method was employed to synthesize ZnO nanoparticles, with zinc acetate as the initial substance. The resulting nanoparticles exhibited a high-quality crystalline structure and a tightly controlled size distribution [9].

2. EXPERIMENTAL METHODS

2.1.ChemicalMaterials

Phenol (C_6H_5OH, molecular weight: 94.11 g/mol) was purchased from Sigma-Aldrich and used as the model pollutant in wastewater. Stock solutions of phenol were prepared by dissolving phenol in deionized water to achieve the desired concentrations. The oxidant used in the oxidation process was hydrogen peroxide (H_2O_2) manufactured by Scharlau (Spain, 35%). ZnO was used as a photocatalyst and was synthesized using the sol-gel method. Three different solvents were employed during the synthesis process to prepare ZnO nanoparticles, Zinc acetate dehydrate (Zn $(CH_3COO)_2 2H_2O$) as a precursor; meanwhile, Glycerol ($C_3H_8O_3$), ethanol (CH_2COOH), and deionized water were used assolvents.

2.2 Preparation methodof photocatalytic ZnO

ZnO nanoparticles were synthesized using the sol-gel method in this study.Zinc acetate dihydrate (Zn $(CH_3COO)_2 \cdot 2H_2O$) was dissolved separately in three solvents: deionized water, ethanol, and glycerol, so-called CAT-1, CAT-2, and CAT-3, respectively. For each solution, a fixed amount of zinc acetate was added to ensure consistency in molar concentration across the solvents. The typical experiment procedure was as follows; 25 grams of zinc acetate dihydrate (Zn $(CH_3COO)_2 \cdot 2H_2O$) was dissolved in three different solventsdeionized water, ethanol, and glycerolusing a weight ratio of 1:3 zinc acetate/solvent (wt/wt), resulting in 75 grams of solvent per 25 grams of zinc acetate. This ratio was chosen to standardize the solvent quantity relative to the amount of zinc acetate and to ensure consistent dissolution conditions across all three solvents.

2.2.1 CAT-1Zinc acetate dehydrate (Zn (CH3COO)2.2H2O) + Deionized water

75 g of deionized water added to 25 g of zinc acetate dehydrate at 80°C with continuous stirring for 90 minutes. then the solution was dried at 80°C for 24 hours.Preparation stages of CAT-1 are described in **Figure 1**

2.2.2 CAT-2Zinc acetate dehydrate (Zn $(CH_3COO)_2.2H_2O$) + Ethanol absolute (CH_2COOH)

International Journal of Environmental Sciences
ISSN: 2229-7359
Vol. 11 No. 1s, 2025
https://www.theaspd.com/ijes.php

75 g of ethanol was added to 25 g of zinc acetate dehydrate and stirred for 2 hoursat 65°C The resultant whitish solution was allowed to gel by aging it for 2 hours and subsequently dried at 65°C in an oven for 24 hours.**Figure 2**described Preparation stages of CAT-2 .

2.2.3 CAT-3Zinc acetate dehydrate (Zn (CH3COO)2.2H2O) + Glycerol ($C_3H_8O_3$)

75 g of glycerol added to 25 g of zinc acetate under vigorous stirring for 48 hours at 150 °C. After the gel formed, it was dissolved by adding ethanol and stirred continuously for another 24 hours. This step helped break down the gel and facilitate the extraction of zinc oxide precursors in a homogeneous solution, and to be ready for subsequent filtration and drying. The mixture was then filtered to eliminate any undissolved particles and impurities. Finally, the filtrate was dried in an oven at 120°C for 24 hours to remove residual ethanol and obtain the zinc oxide precursor.The steps of the method were illustrated in **Figure 3.**

However,each sample was subjected to calcination at four different temperatures,300°C, 400°C, 500°C, and 600°C,in a tubular furnace. The samples were heated gradually to the target temperature and held for 4 hours to ensure complete transformation of the precursor gel to zinc oxide

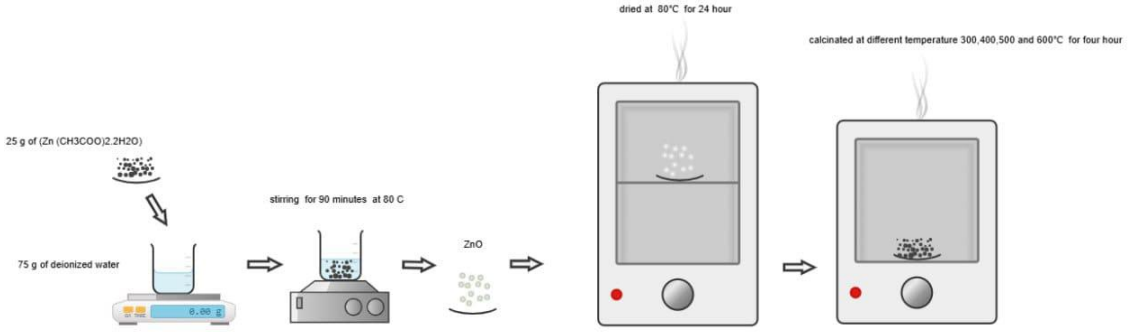

Figure 1. ZnO with Water

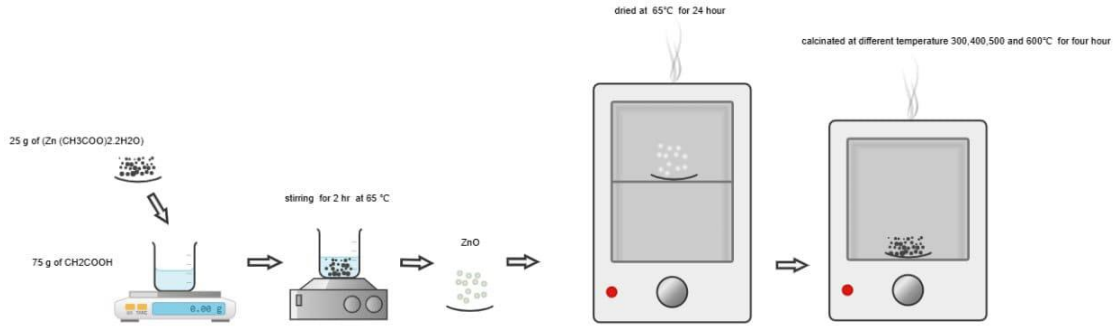

Figure 2. ZnO with ethanol

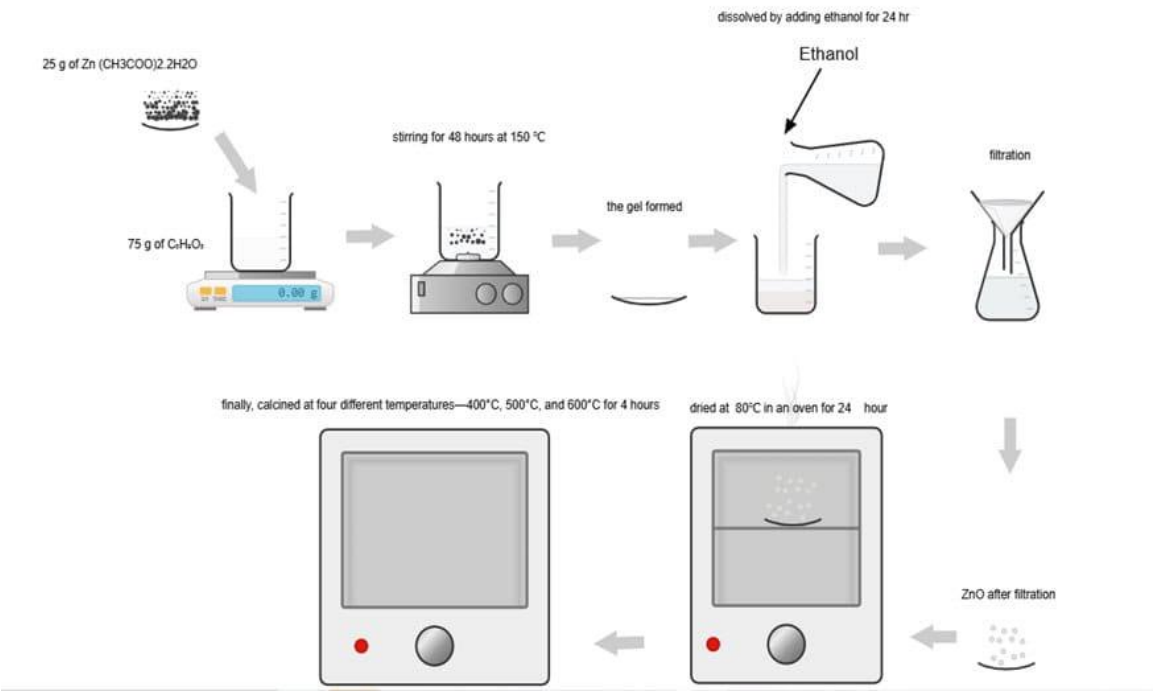

Figure 3. ZnO with Glycerol

2.3 Experimental setup

A series of batch experiments were conducted to study the phenol removal kinetics using a home-made photocatalytic reactor with a length of 60 cm, a depth of 42 cm, and a height of 37 cm. The reactor was equipped with eight UV lamps of 6W Philips, a cooler fan of 10 cm diameter, and a vacuum fan of 10 cm diameter, as illustrated in its schematic diagram in Figure 4. Stock solutions of phenol were prepared by dissolving pure phenol (C_6H_5OH) in deionized water to achieve the desired initial concentrations of 50 ppm, 100 ppm, 150 ppm, and 200 ppm. Four different doses of photocatalyst were tested to evaluate their effect on the degradation rate: 0.05, 0.1, 0.15, and 0.2 g/100 mL. The mixture was stirred and irradiated with UV light for 180 minutes. At regular intervals, 50 mL of the solution was taken, and the reactor was filled with the prepared phenol solution and slurry. The UV lamp was turned on, and the system was allowed to operate for 3 hours under constant air flow (2 L/min). During this period, samples of the solution were taken at regular time intervals (5, 10, 20, 30, 60, 90,120,180 minutes) to measure the residual phenol concentration. After each sampling period, the phenol concentration was determined by High-Performance Liquid Chromatography (HPLC). The effectsof contact time, photocatalyst dosage, and the initial concentration of phenol on photo catalytic degradation of phenol were investigated. The phenol removal efficiency was calculated at different time intervals using eq (1):

$$\text{Removal efficiency } (\alpha) = \frac{C_0 - C_t}{C_0} * 100 \quad (1)$$

Where:

- C_0 is the initial phenol concentration (ppm).
- C_t is the phenol concentration at time t (ppm)

International Journal of Environmental Sciences
ISSN: 2229-7359
Vol. 11 No. 1s, 2025
https://www.theaspd.com/ijes.php

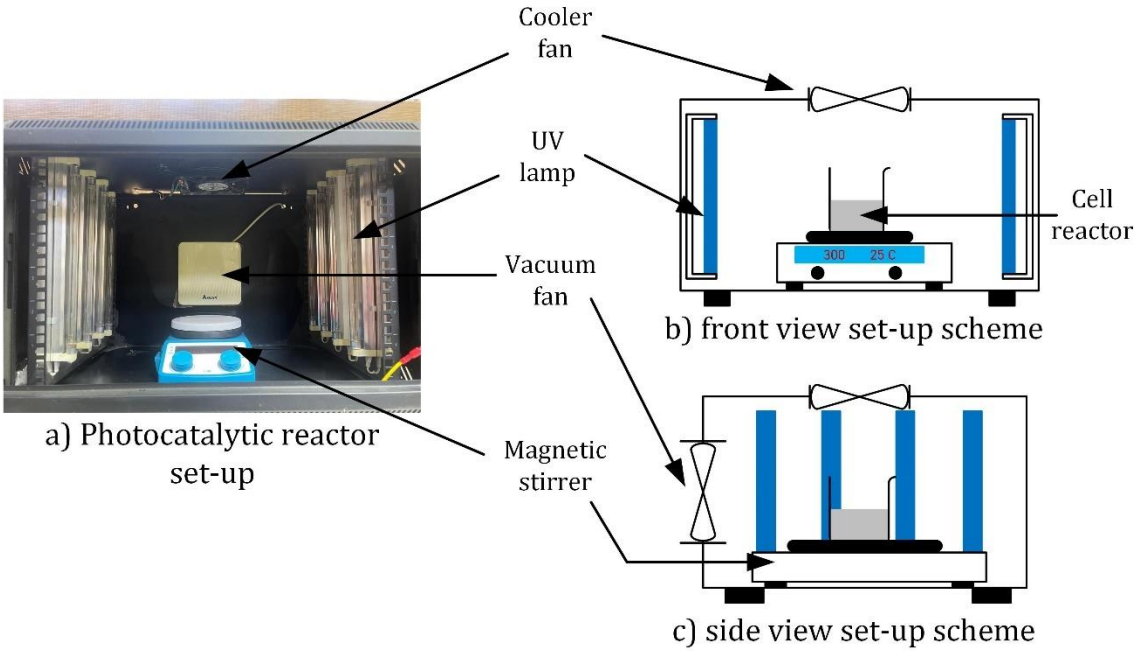

Figure 4. Reactor setup

2.4 Characterization of ZnO nanoparticles

The characterization of synthesized nanoparticles was conducted using several analytical techniques including X-ray diffraction (XRD) that was performed to analyze the crystal structure and phase purity of the ZnO nanoparticle and this characterization of ZnO using X-ray diffraction was conducted with filtered Cu Kα radiation at 40 kV and 20 mA, SEM (A scanning electron microscope) was utilized to analyze the surface morphology, particle size, and dispersion of the produced ZnO nanoparticles. This approach yields high-resolution images that facilitate the analysis of particle morphology and structural consistency. Fourier Transform Infrared Spectroscopy (FTIR) is a method that uses absorption to analyze a sample's infrared spectrum. FTIR characterization was conducted to confirm the presence of zinc and oxygen atoms in the synthesized zinc oxide nanoparticles. Furthermore, identify any other functional groups that might be present. Comprehending the decomposition characteristics of ZnO precursors facilitates the enhancement of the calcination procedure to get stable, high-purity ZnO nanoparticles

2.5Kinetic of photocatalytic degradation phenol

The photocatalytic degradation of phenol was analyzed to determine the reaction kinetics and to investigate the rate at which phenol was removed under UV irradiation using ZnO as a photocatalyst. Initially, a portion of phenol undergoes oxidation through a direct interaction with the active holes on the catalyst (ZnO) surface, resulting in the formation of intermediates that can further react to produce the final products. The reaction mechanism for this process is effectively explained by the Langmuir–Hinshelwood kinetics, where phenol molecules are first adsorbed onto the catalyst surface and then proceed to react according to a first-order reaction[33].so, The degradation data were found to follow pseudo-first-order kinetics, which is commonly observed in photocatalytic processes.

$$-r_{ph} = -\frac{dC_{ph}}{dt} = k_{app} C_{phenol} \quad (2)$$

It has been assumed that the order is first-order rate equation (n=1)

$$\frac{dC}{dt} = -k1 * C = K_{app} C_{ph} \quad (3)$$

By separation of variables and integration of equation , we obtain

$$Ln\left(\frac{C_{phenol}}{C_{phenl\ ,0}}\right) = -k_{app} * t \quad (4)$$

Where:

- K app represents the apparent pseudo first order reaction rate constant
- C_{phenol} is the phenol concentration (mg/L) at any time
- $C_{phenl\ ,0}$ is the initial concentration of phenol
- t is the time (min).

The calculated result indicated that phenol photocatalytic degradation at the reaction conditions follows a pseudo-first-order kinetics

3. RESULTS AND DISCUSSION

3.1 X-ray diffraction analysis

The samples were scanned over 2θ angles (20° to 80°). CuK radiation was used for the measurements, which were carried out at 40 kV and 40 mA. displays the X-ray diffraction pattern of the ZnO nanoparticles synthesized in this study [34]. X-ray diffraction (XRD) analysis was performed on ZnO samples calcined at various temperatures (400°C, 500°C, and 600°C) to examine the impact of temperature on crystallinity and phase purity.**Figure 5**showsthe XRD characteristic peaks of CAT 1_ 400that align with the known diffraction pattern of zinc oxide (ZnO), specifically with the wurtzite hexagonal structure.**Figure 6**depicts amplification of the peak at roughly 36° of the (101) ZnO crystal plane, accompanied by a slight shift to a lower angle. This result indicates a change in the lattice properties and cell volumes of the hexagonal structure of ZnO [35]. The (101) plane had the highest relative intensity in all XRD patterns, signifying anisotropic growth and a preferred orientation of the crystallites [36].

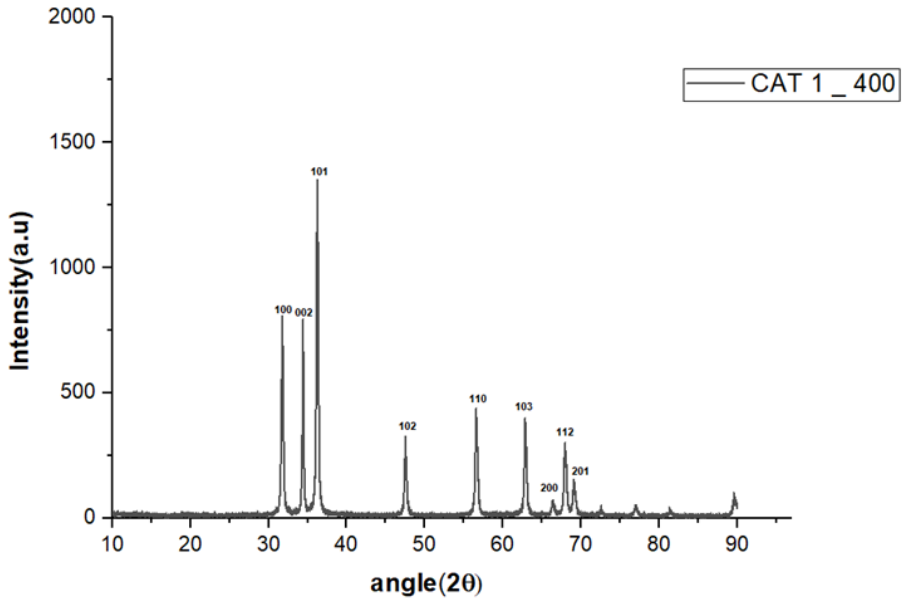

Figure 5. XRD pattern of CAT_1 at 400°C

This XRD pattern likely indicates a well-crystallized ZnO phase devoid of notable secondary phases. The sample exhibits pronounced peaks at ZnO's characteristic 2θ values, signifying a wurtzite crystal structure and high crystallinity, especially at the 400°C synthesis temperature. To calculate the crystallite size for this sample from X-ray diffraction (XRD), we can use the Scherrer Equation eq (2)

$$D = (k\lambda)/(\beta \cos\theta) \quad (2)$$

Where:

D = Crystallite size (in nanometers, nm)

λ = X-ray wavelength (1.5406 Å for Cu Kα alpha α radiation)

k = the Scherer constant = (0.89)

β = Full Width at Half Maximum (FWHM) of the peak in radians (corrected for instrumental broadening)

θ = Bragg angle of the peak (half of the 2θ value in degrees, converted to radians).

The peak near 2θ ≈ 36° might be a good choice, and FWHM in degrees = 0.2°, after applying the Scherrer Equation. For this peak crystallite size of the sample is D≈40.3 nm. Figure 6shows the XRD pattern of ZnO nanoparticles.All samples of zinc oxide showed broad peaks in the 2θ range around 31°, 34°, 36°, 47°, and 56° are typical for the hexagonal wurtzite structure of ZnO. These peaks correspond to specific crystal planes, like (100), (002), (101), (102), and (110), respectively, which are commonly observed in ZnO. No additional peaks associated with impurities were observed, indicating the acquisition of high-purity ZnO nanoparticles and The optimal calcination temperature are 400 degrees Celsius because the major peak at these temperatures is sharper and their full-width at half maximum (FWHM) is smaller, which corresponds to 500 and 600 degrees Celsius [37]. The similarity in peak positions across all samples suggests that all of these materials have a similar ZnO crystalline phase, likely wurtzite. As the calcination temperature increases (from 400°C to 600°C),

the peaks generally become sharper and more intense. This trend suggests improved crystallinity at higher calcination temperatures, as higher temperatures typically promote crystal growth and reduce defects.We also notice there is a noticeable decrease in peak width with increased calcination temperature. Narrower peaks at higher temperatures (such as 600°C) indicate larger crystallite sizes due to grain growth during the calcination process.

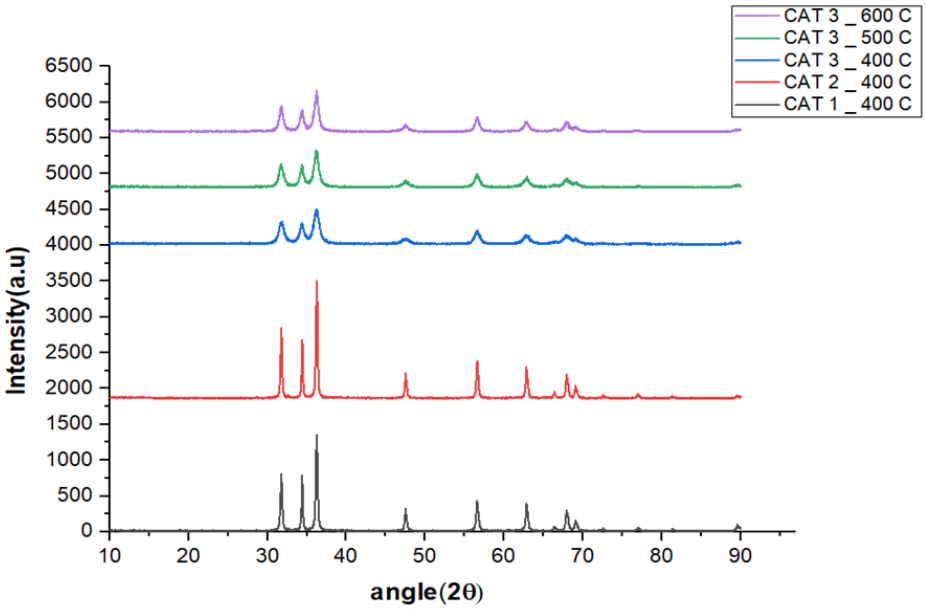

Figure 6. XRD pattern of ZnO nanoparticles

3.2 Fourier transform infra-red (FTIR) spectra

The FTIR spectra of ZnO nanoparticles calcined at various temperatures (400 °C, 500 °C, and 600 °C) are presented in**Figure 7.**The fingerprint bands detected at 641 cm^{-1} and 831 cm^{-1} correspond to the interatomic vibrations of the Zn–O link. These bands are indicative of zinc metal, as metallic bands are often detected below 1000 cm^{-1}. The peak at 1428 cm^{-1} is attributed to the stretching vibration of the C-N bond in primary amines or the C-O bond in primary alcohols. The peak at 1562 cm^{-1} is linked to the in-plane bending or vibration of primary alcohol. The peaks at 3321.42 cm^{-1} and 3533.59 $cm^{-1}$are attributable to O–H (hydroxyl group) bond stretching and deformation resulting from water molecules adsorbed on the surface of zinc [38] Bands stretching at ~1650 cm^{-1}, This corresponds to O–H bending vibrations from adsorbed water molecules . The O = C = O vibration of the CO2 molecule present in the air is represented by a band around 2153.75 cm^{-1}[39]. The bands observed between ~1400–1450 cm^{-1} this peak may be attributed to C–O stretching vibrations or carbonate species (CO_3^{2-}). These can form due to atmospheric CO_2 reacting with the surface of ZnO or residual precursors during synthesis

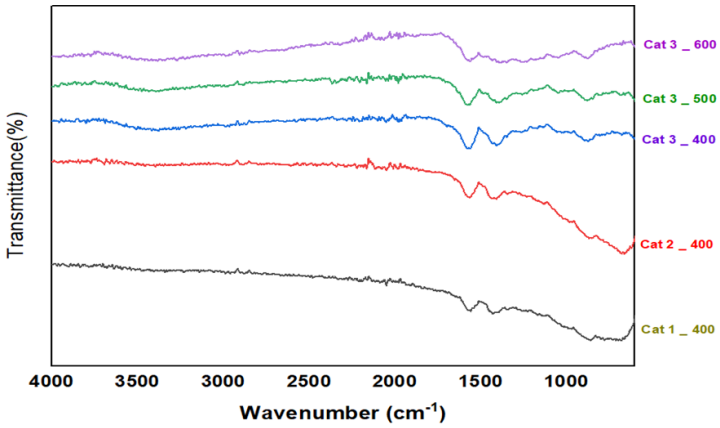

Figure 7. FTIR spectra of ZnO nanoparticles

3.3 Scanning electron microscopy (SEM)

This method uses a concentrated electron beam to scan the surface of the sample, and interactions between the sample and the beam provide high-resolution pictures that show nanoscale surface details. The SEM investigation was performed at an accelerating voltage of 15 kV, with pictures obtained at magnifications ranging from 10,000× to 50,000×. **Figure 8** illustrates the SEM images of ZnO synthesized through the sol-gel method at 400°C by three different solvents. As shown in**Figure 8**, ZnO is seen to have pseudo-spherical forms, with some distinctly rod-like. Additionally, it was noted that the particle formation occurs structurally disorganized. Some of the particles resemble lengthy rods, while others like large, short rods. ZnO particles range in size from 20 to 140 nm. The development of crystallites may be the cause of the large variety of particle sizes. The size of the particles will be influenced by the crystallite development on the ZnO surface. Therefore, the size of the resulting ZnO was significantly influenced by the chemical composition used for its manufacture. [40]

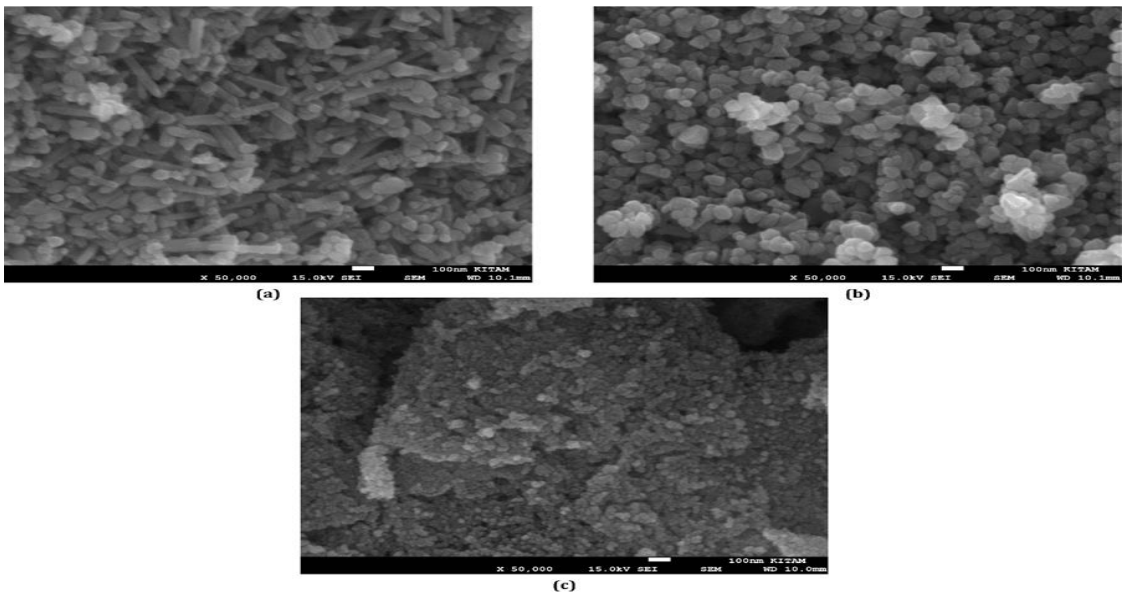

Figure 8. SEM image of ZnO nanoparticles calcined at 400 °C: a) zinc oxide synthesized by deionized water as a solvent, b) zinc oxide synthesized by ethanol as a solvent, c) zinc oxide synthesized by glycerol as a solvent

At 400°C, the ZnO nanoparticles have undergone enough crystallization to form stable, uniform particles without excessive growth or sintering, resulting in good crystallinity and surface stability. This temperature promotes a balance between surface area and particle stability, making it ideal for maintaining nanoscale particles without significant fusion. **Figure 8-a**shows ZnO nanoparticles prepared using water, with a distinct rod-like or needle-shaped form. This elongated form indicates anisotropic growth, perhaps affected by synthesis conditions and the moderate calcination temperature, which aids in stabilizing the rod shape. The rods seem slender, exhibiting a significant aspect ratio. Although precise dimensions are not provided, they are likely between 10 and 30 nm in width and may stretch to several hundred nanometers in length, as inferred from the scale bar, Furthermore, because of their one-dimensional nanostructures (such as nanorods and nanotubes), which can enable more effective carrier transport due to a reduction in grain borders, surface flaws, disorders, and discontinuous interfaces, rod-like structures are the best nanostructures when compared to others [41]. **Figure 8-b**displays the SEM micrograph ofZnO nanoparticles prepared using ethanol, characterized by an average particle size of 17.5 ± 5 nm, exhibiting homogenous and hexagonal forms with significant agglomeration [42].And shows granular or nearly spherical ZnO nanoparticles that are densely packed. The particles appear to be small and somewhat uniform, with some degree of aggregation. The image above displays densely packed ZnO nanoparticles that are granular or almost spherical. The particles measure between 20 and 50 nm in diameter, typical of ZnO calcined at 400°C, a temperature sufficient to commence crystallization without promoting significant particle development.**Figure 8-c**shows ZnO nanoparticles prepared using glycerol, densely packed, spherical ZnO nanoparticles with a more uniform size distribution than in the second image. The particles are small and closely aggregated, which can be typical for ZnO calcined at a controlled temperature like 400°C and particles appear to be within the 20 to 40 nm range, and their uniformity suggests controlled nucleation and growth during synthesis and calcination.

3.4 Brunauer–Emmet–Teller (BET) specific area analysis

BET analysis was used to investigate the surface structure of synthesized ZnO NPs, **Table 1** Summarizes the characteristics of the Zinc oxide nanoparticles synthesized using different solvents (water, ethanol, and glycerol) at a temperature of 400°C for 4 hours are shown in **Table 1.**

Table 1. BET analysis data

No.	Solution	Temperature (C)	Time (h)	Surface area (m^2/g)	Pore volume (cm^3/g)	Pore radius (nm)
1.	Water	400	4	14.6064	0.070844	1.74595
2.	Ethanol	400	4	11.914	0.0695245	1.61556
3.	Glycerol	400	4	36.357	0.183393	8.47117

The ZnO particles produced with glycerol demonstrated a significantly larger surface area of 36.357 m^2/g, with a pore volume of 0.183393 cm^3/g and a larger pore radius of 8.47117 nm, The results suggested that glycerol is the most effective solvent in terms of enhancing the surface area, pore volume, and pore radius of the ZnO nanoparticles.These properties are important for the photocatalytic process, as larger surface areas and larger pores provide more active sites and better

access to the reactants, improving the catalyst's performance Water and ethanol, while still effective, yield ZnO with smaller surface areas and pore volumes, which might limit their efficiency in certain catalytic processes. Thus, ZnO synthesized with glycerol would likely perform better in photocatalytic applications (such as phenol degradation from wastewater) due to its higher surface area and larger pores, which are essential for effective photocatalysis.

3.5 Effect of Catalyst Type

In this study, ZnO nanoparticles were synthesized using the sol-gel method using three different solvents: water, ethanol, and glycerol. Their photocatalytic activity was tested in the degradation of phenol in aqueous solutions under UV light. The results showed that the solvent used during synthesis had a significant impact on the particle size, crystallinity, and photocatalytic efficiency of ZnO, as shown in **Figure 9** ZnO synthesized in glycerol exhibited the highest phenol removal efficiency (100%) after 60 minutes of UV irradiation, followed by ethanol (93.50 %) and deionized water (85%). Based on the experimental results, glycerol proved to be the best solvent for synthesizing ZnO nanoparticles for photocatalytic phenol removal. The uniform morphology, high crystallinity, and small particle size of the ZnO synthesized in glycerol contributed to its superior photocatalytic performance, with a 100% phenol removal efficiency after only 60 minutes of UV irradiation.

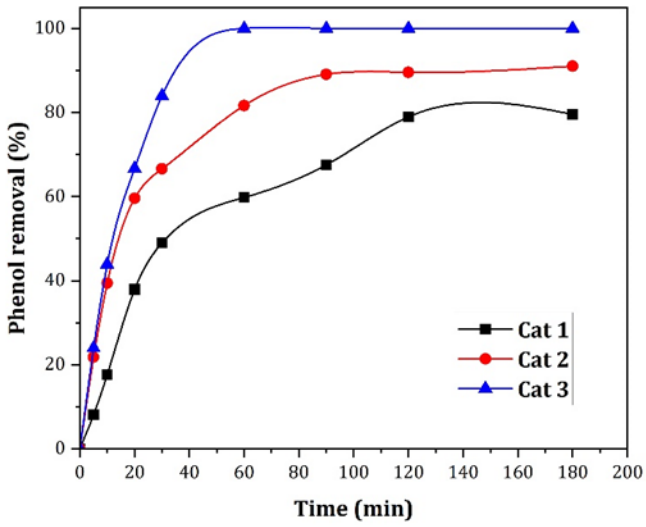

Figure 9. Effect of the typeof catalyst

The unique properties of glycerol, such as its high viscosity and ability to stabilize ZnO nanoparticles, were key factors that made it a better choice than water or ethanol. Additionally, glycerol has hydroxyl groups that may interact with the Zn precursor during sol-gel synthesis, promoting the formation of well-structured ZnO nanoparticles. Because glycerol has three hydroxyl groups, using it as a solvent can shorten the time it takes for the atoms to react to produce nanoparticles. Additionally, it can accelerate the production of gels, and the heat produced by the chemical reaction can speed up the rate of reaction[43]. The interaction between glycerol and the zinc precursor could also play a role in stabilizing smaller ZnO particles, which would not be as easily achieved with water or ethanol. While water is a commonly used solvent due to its availability and low cost, ZnO synthesized in water showed lower photocatalytic efficiency compared to glycerol. This is likely due to larger particle size

and less uniform dispersion, which limited the surface area available for phenol adsorption and degradation. Similarly, although ethanol typically produces ZnO with smaller particles than water, it did not exhibit the same level of crystallinity or uniformity as glycerol. This suggests that glycerol's unique properties allow for better control over the synthesis of ZnO with high crystallinity and small particle size, which translates to better photocatalytic efficiency. This study suggests that glycerol-based ZnO could be an efficient and stable photocatalyst for environmental applications, particularly for the degradation of phenolic compounds in wastewater. These findings highlight the importance of solvent selection in optimizing the photocatalytic performance of ZnO for environmental applications."

3.6 Effect of calcination temperature

The photocatalytic efficacy of ZnO catalysts synthesized via the sol–gel technique at varying calcination temperatures was evaluated for the photodegradation of phenol under UV light. Various parameters, such as crystal composition and crystal phase, influence the photocatalytic efficacy of ZnO. The photocatalytic activity of ZnO nanoparticles was significantly affected by the calcination temperature. ZnO calcined at 400°C showed the highest phenol removal efficiency (100%) after 60 minutes only of UV exposure. At lower calcination temperatures (300°C), the efficiency was 100% after 90 minutes, while ZnO calcined at 500°C and at 600°C reached 100% removal efficiency after 2 hr., as shown in **Figure 10**. From Figure 10,CAT 3_400°C shows the fastest phenol removal rate, indicating that ZnO synthesized at this temperature has the best combination of properties for photocatalysis.

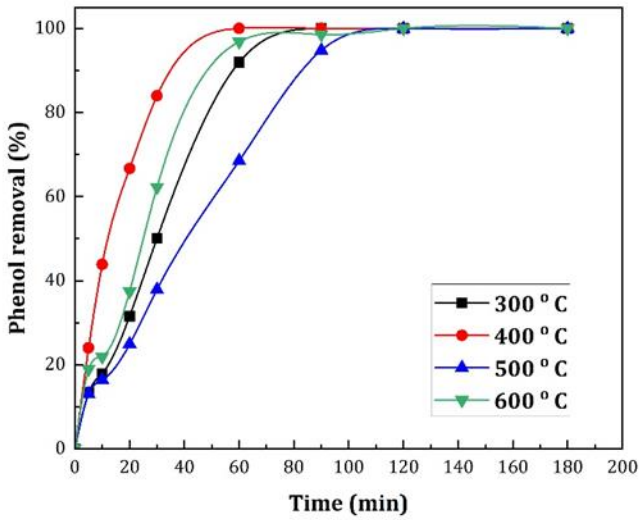

Figure 10. Effect of calcination temperature

3.7 Effect of time calcination

Figure 11observes that 4 hours of calcination yielded the highest phenol removal efficiency. This is because at this point, the material has achieved the optimal surface area and porosity for adsorption. Shorter calcination times did not allow enough time for the material to fully activate, while longer calcination times caused sintering and reduced the number of available active sites.

Therefore, 4 hours provided the best balance between activation and material stability, resulting in the most effective phenol removal."

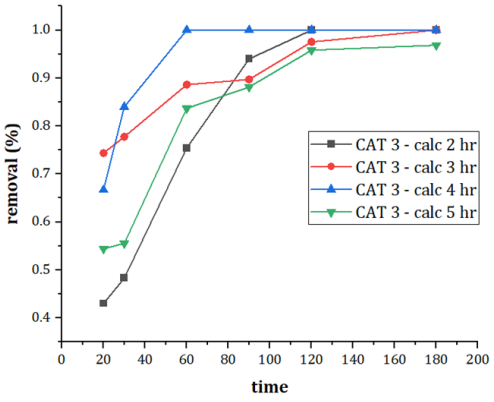

Figure 11. Effect of time calcination

3.8 The Effect of Time on PhotocatalyticDegradation of Phenol

The effect of contact time on phenol removal by oxidation is a critical factor in determining the efficiency of the removal process. **Figure 12** shows the effect of contact time on the phenol photodegradation from the aqueous solutions in the concentration range 50, 100, 150, and 200 ppm, and the catalyst weightsare 0.05, 0.1,0.15, and 0.2 g.As the duration of time increased, the phenol oxidation process was gradually enhanced[44].

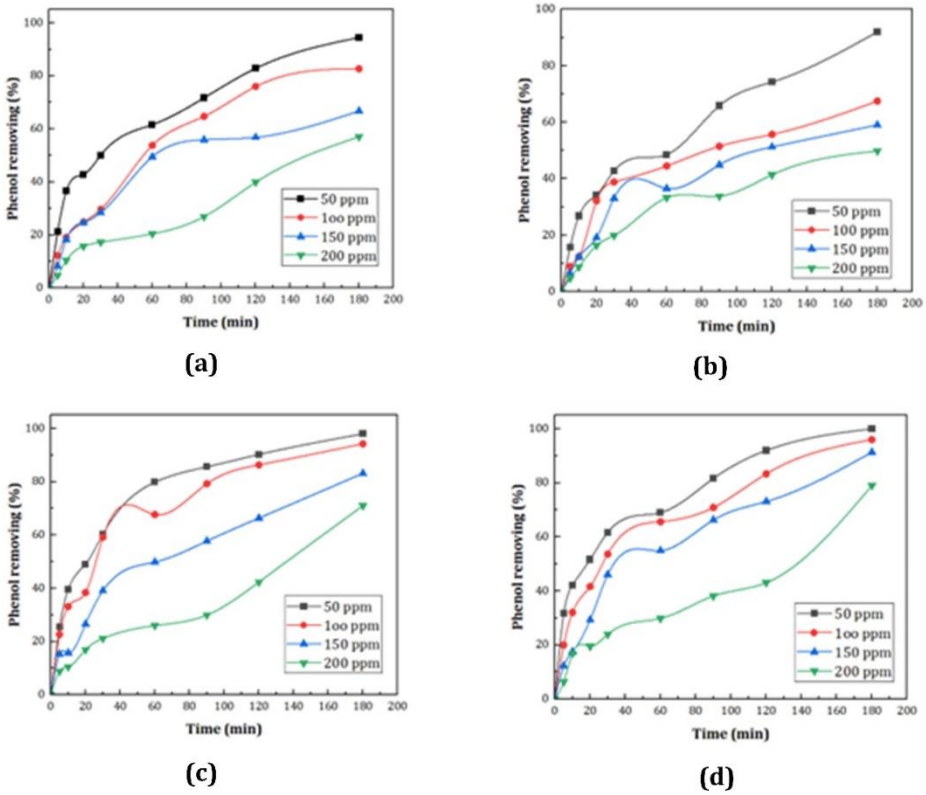

Figure 12. effect contact time on phenol removal at a) 0.05 g/L b) 0.1 g/L c) 0.15 g/L d) 0.2 g/L

In **Figure 12**, it was inferred that phenol removal increases with an increase in contact time. The graph shows that as the contact time increases, the percentage of phenol removal increases for all concentrations (50 ppm, 100 ppm, 150 ppm, and 200 ppm). This suggests that longer contact time enhances the phenol removal process, likely due to more time for the removal mechanism to take effect, whether through adsorption, chemical reactions, or other processes. However, the rate of increase in phenol removal tends to slow down as the contact time continues, indicating that the system might approach a saturation point after a certain period.

Additionally, higher concentrations of phenol (such as 100 ppm, 150 ppm, and 200 ppm) generally show slower removal rates compared to lower concentrations (50 ppm), implying that the phenol removal process becomes less efficient as the phenol concentration increases. Longer contact times allow for more complete reactions, leading to higher phenol removal efficiencies and Sufficient contact time ensures complete reactions, minimizing residual phenol concentrations

3.9 The effect of initial concentrations

The effect of initial concentrations of phenol on the phenol removal was also shown in figure 13 , the removal rate of phenol decreases, with an increase in initial concentration of phenol, Specifically, for all the different adsorbent doses (0.05 g/100 mL, 0.1 g/100 mL, 0.15 g/100 mL, and 0.2 g/100 mL), phenol removal efficiency declines as the initial concentration rises from 50 ppm to 200 ppm. This trend suggests that a higher initial phenol concentration may overwhelm the available active sites on the adsorbent, leading to reduced efficiency in phenol removal. At higher concentrations, the adsorbent becomes less efficient in phenol removal, likely due to saturation or a shortage of available binding sites. As the concentration of the pollutant rises, a greater number of pollutant molecules are adsorbed onto the surface of the semiconductor, reducing the overall efficiency of the process[45], An increase in the initial concentration of the organic compound lowers the efficiency of photocatalyst degradation. This can be attributed to the fact that higher concentrations lead to more molecules adsorbing onto the surface of the photocatalyst. As a result, there is less available surface area for the formation of hydroxyl radicals, which in turn diminishes the photocatalytic activity of the catalyst [46].

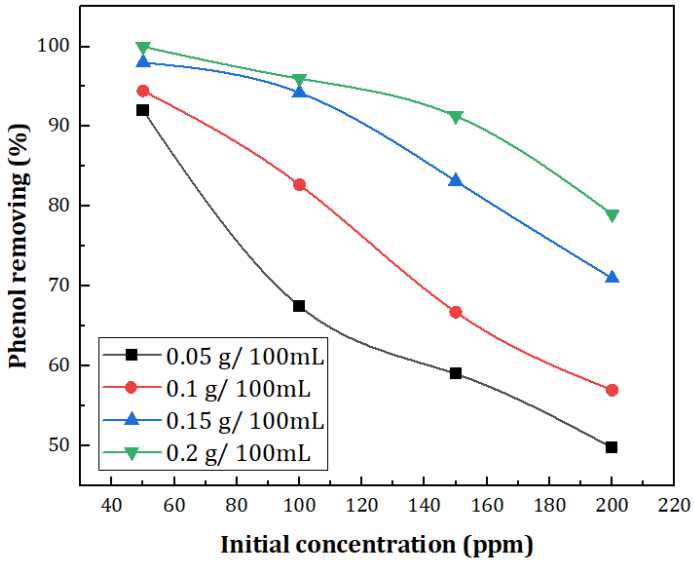

Figure 13.Effect of initial concentration

International Journal of Environmental Sciences
ISSN: 2229-7359
Vol. 11 No. 1s, 2025
https://www.theaspd.com/ijes.php

3.10 The effect of the catalyst's dose

The amount of catalyst influences the reaction rate, providing a surface for adsorption and generating oxidative holes in the valence band and electrons [33]. Various experiments were performed to evaluate the impact of catalyst loading on the reaction rate, with catalyst loadings ranging from 0.05 to 0.2 g/L. Figure 14shows that increasing the catalyst dose leads to higher phenol removal efficiency. As the weight of the catalyst increases, the percentage of phenol removal improves for all concentrations (50 ppm, 100 ppm, 150 ppm, and 200 ppm). The increase in ZnO nanoparticle dosage from 0.05 to 0.2 g/L increases the removal of phenol. This suggests that a higher catalyst dose provides more active sites for adsorption and photocatalytic reactions, thus enhancing the removal of phenol from the solution. However, this effect seems to plateau at higher catalyst doses, as the phenol removal rate increases more slowly after a certain point, indicating that further increases in catalyst weight may not significantly enhance the removal efficiency.at At 200 ppm, the graph shows that increasing the catalyst dose leads to a noticeable improvement in phenol removal.

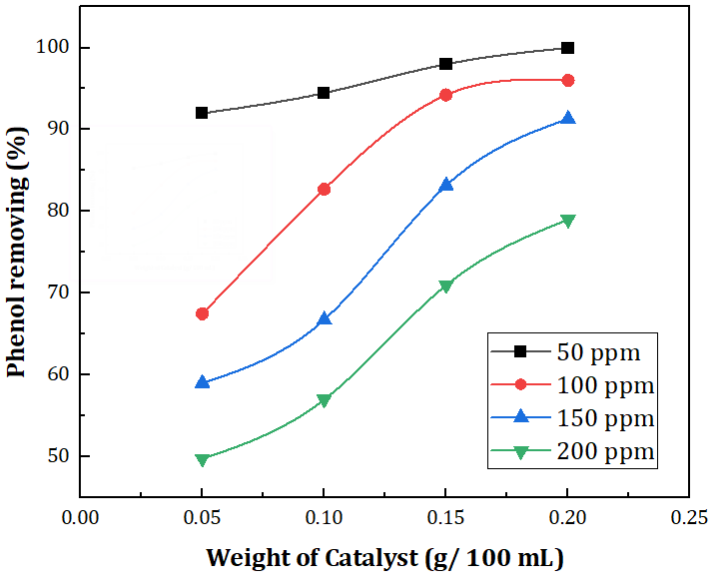

Figure 14. Dose effect on phenol removal

As the weight of the catalyst increases from 0.05 g/100 mL to 0.2 g/100 mL, the phenol removal efficiency increases from approximately 65% to around 85%. This indicates that a higher catalyst dose enhances the removal of phenol from the solution at 200 ppm. However, the increase in phenol removal becomes less pronounced at higher catalyst doses, suggesting there is a limit to the benefit of increasing the catalyst weight at this high concentration.

3.11 The effect of initial concentration on kinetic

The plot of ln (Cphenol/Cphenol,0) versus time for all the experiments with different initial concentrations of phenol is shown in **Figure 15**. The values of Kapp were obtained directly from the regression analysis of the linear curve in the plot, further validating the first-order. Results showed that K_{app} decreased when the phenol initial concentration increased, as shown in Table 2. The rate of a unimolecular surface reaction is directlyproportional to the surface coverage, assuming that the reactant is more strongly adsorbed on the catalyst surface than the products[47].

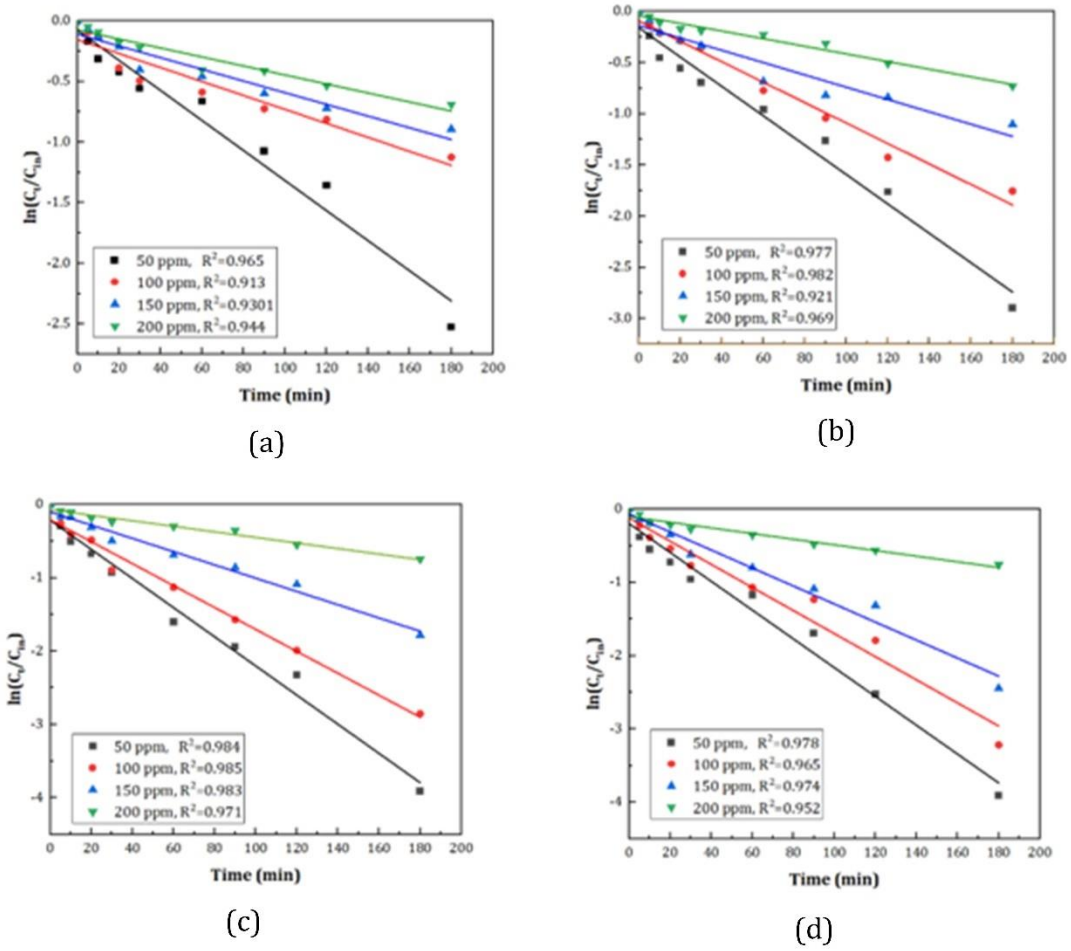

Figure 15. Effect of initial phenol concentration:a) initial concentration 50 ppm b) initial concentration 100 ppm c) initial concentration 150 ppm d) initial concentration 200 ppm

Table 2. Regression coefficients (R2) and Kapp for the effect of initial concentrations on kinetics for phenol photo degradation

		Dose of catalyst			
		0.05 g/L	**0.1 g/L**	**0.15 g/L**	**0.2 g/L**
C0					
50 ppm	R^2	0.965	0.977	0.984	0.978
	K_{app}	0.0124	0.0143	0.0199	0.019
100 ppm	R^2	0.913	0.982	0.985	0.965
	K_{app}	0.0058	0.01	0.0149	0.0158
150 ppm	R^2	0.9301	0.921	0.983	0.974
	K_{app}	0.0048	0.006	0.009	0.0123
200 ppm	R^2	0.944	0.969	0.971	0.952
	K_{app}	0.0037	0.0037	0.0038	0.0039

International Journal of Environmental Sciences
ISSN: 2229-7359
Vol. 11 No. 1s, 2025
https://www.theaspd.com/ijes.php

3.12 The effect of the dose of the catalyst on kinetics

The Dose effect on kinetics in photocatalytic degradation using ZnO shows that the reaction rate increases with catalyst dose up to an optimal point. After this optimal dose, increasing the catalyst concentration leads to diminishing returns due to saturation, light scattering, and surface aggregation. Therefore, there is a balance between the amount of catalyst used and the efficiency of the degradation process, where too much catalyst beyond a certain level doesn't improve performance and may even hinder it. Figure 16 andTable 3showthe effectof the dose of the catalyst on kinetics.

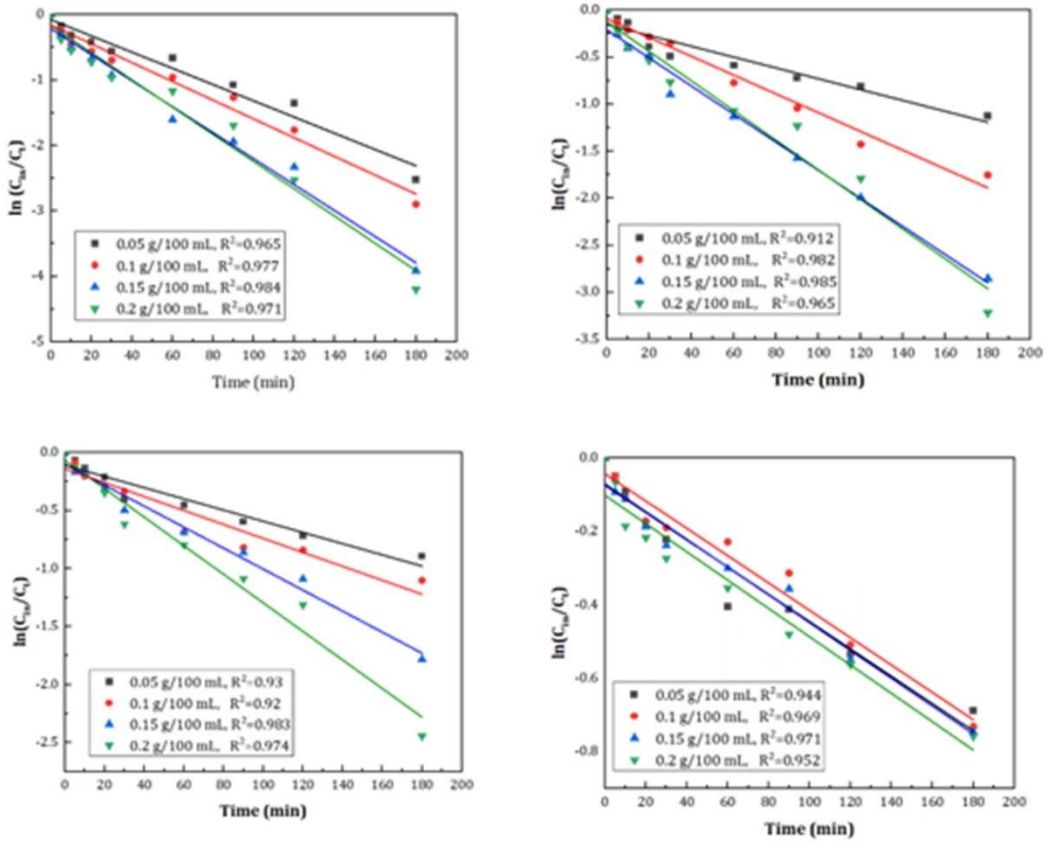

Figure 16. Effect of dose catalyst on Kineticsa) weight of Catalyst 0.05 g/L, b) weight of Catalyst 0.1 g/L, c) weight of Catalyst 0.15 g/L, d) weight of Catalyst 0.2 g/L

Table 3. Regression coefficients (R2) and Kapp for Dose effect on kinetics for phenol photo degradation

		C0			
		50 ppm	**100 ppm**	**150 ppm**	**200 ppm**
Dose of cat.					
0.05 g/L	R^2	0.965	0.912	0.93	0.944
	K_{app}	0.0124	0.0058	0.0048	0.0037
0.1 g/L	R^2	0.977	0.982	0.92	0.969
	K_{app}	0.0143	0.01	0.006	0.0037
0.15 g/L	R^2	0.984	0.985	0.983	0.971
	K_{app}	0.0199	0.0149	0.009	0.0038
0.2 g/L	R^2	0.971	0.965	0.974	0.952
	K_{app}	0.02	0.0158	0.0123	0.0039

CONCLUSIONS

ZnO nanoparticles were successfully synthesized and used in this study to photocatalytically degrade phenol from industrial effluent. ZnO was created using a sol-gel method and three distinct solvents: glycerol (CAT-3), ethanol (CAT-2), and deionized water (CAT-1). Superior photocatalytic activity was a result of the largest surface area and crystallinity of CAT-3 (glycerol-based ZnO) calcined at 400°C. In a UV-assisted slurry bubble column reactor, the ZnO catalysts were used to break down phenol mostly by producing reactive radicals (•OH, $•O_2^-$) through UV-induced electron–hole separation. Over 90% phenol removal efficiency was attained with CAT-3 under ideal conditions (0.15 g/L catalyst dosage, 100 ppm phenol concentration, and 180 minutes of irradiation).

The results highlight the importance of solvent selection in ZnO synthesis and validate the potential of UV/ZnO systems for sustainable and efficient water treatment applications. Future work may focus on reactor scale-up, catalyst stability, and degradation pathways of by-products.

REFERENCES

[1] M. Said, "Removal Methods Phenol From water Some methods and technologies used today are described below :," 2021.

[2] R. Thiruvenkatachari, S. Vigneswaran, and I. S. Moon, "A review on UV/TiO2 photocatalytic oxidation process," *Korean J. Chem. Eng.*, vol. 25, no. 1, pp. 64–72, 2008, doi: 10.1007/s11814-008-0011-8.

[3] G. Boczkaj and A. Fernandes, "Wastewater treatment by means of advanced oxidation processes at basic pH conditions: A review," *Chem. Eng. J.*, vol. 320, pp. 608–633, 2017, doi: 10.1016/j.cej.2017.03.084.

[4] D. Alhaddad, F. Kndil, and A. Falah, "Preparation and Characterization of Zinc Oxide Nanoparticles via the Thermal Decomposition," *Nanosistemi, Nanomater. Nanotehnologii*, vol.

19, no. 4, pp. 855–863, 2021, doi: 10.15407/nnn.19.04.855.

[5] P. Shafiee, M. Reisi Nafchi, S. Eskandarinezhad, S. Mahmoudi, and E. Ahmadi, "Sol-gel zinc oxide nanoparticles: advances in synthesis and applications," *Synth. Sinter.*, vol. 1, no. 4, pp. 242–254, 2021, doi: 10.53063/synsint.2021.1477.

[6] X. Zhang *et al.*, "Carbon-Doped ZnO Nanostructures: Facile Synthesis and Visible Light Photocatalytic Applications," *J. Phys. Chem.* C, vol. 119, no. 35, pp. 20544–20554, 2015, doi: 10.1021/acs.jpcc.5b07116.

[7] Y. Y. Kedruk *et al.*, "Morphology Effects on Electro- and Photo-Catalytic Properties of Zinc Oxide Nanostructures," *Nanomaterials*, vol. 13, no. 18, 2023, doi: 10.3390/nano13182527.

[8] A. Kolodziejczak-Radzimska and T. Jesionowski, "Zinc oxide-from synthesis to application: A review," *Materials (Basel).*, vol. 7, no. 4, pp. 2833–2881, 2014, doi: 10.3390/ma7042833.

[9] M. M. Ba-Abbad, A. A. H. Kadhum, A. Bakar Mohamad, M. S. Takriff, and K. Sopian, "The effect of process parameters on the size of ZnO nanoparticles synthesized via the sol-gel technique," *J. Alloys Compd.*, vol. 550, pp. 63–70, 2013, doi: 10.1016/j.jallcom.2012.09.076.

[10] T. Nagase, T. Ooie, and J. Sakakibara, "Novel approach to prepare zinc oxide films: Excimer laser irradiation of sol-gel derived precursor films," *Thin Solid Films*, vol. 357, no. 2, pp. 151–158, 1999, doi: 10.1016/S0040-6090(99)00645-8.

[11] M. Jyoti, D. Vijay, and S. Radha, "To Study the Role of Temperature and Sodium Hydroxide Concentration in the Synthesis of Zinc Oxide Nanoparticles," *Int. J. Sci. Res. Publ.*, vol. 3, no. 11, pp. 2250–3153, 2013, [Online]. Available: www.ijsrp.org

[12] M. Ristić, S. Musić, M. Ivanda, and S. Popović, "Sol-gel synthesis and characterization of nanocrystalline ZnO powders," *J. Alloys Compd.*, vol. 397, no. 1–2, pp. 4–7, 2005, doi: 10.1016/j.jallcom.2005.01.045.

[13] M. K. Hossain, S. C. Ghosh, Y. Boontongkong, C. Thanachayanont, and J. Dutta, "Growth of Zinc Oxide nanowires and nanobelts for gas sensing applications," *J. Metastable Nanocrystalline Mater.*, vol. 23, pp. 27–30, 2005, doi: 10.4028/www.scientific.net/JMNM.23.27.

[14] N. Paper and P. Submission, "Synthesis of Zinc Oxide Nanoparticles via Sol – Gel Route and Their Characterization Synthesis of Zinc Oxide Nanoparticles via Sol – Gel Route and Their Characterization Synthesis of Zinc Oxide Nanoparticles via Sol – Gel Route and Their Characterization," vol. 5, no. 2009, pp. 2010–2014, 2016, doi: 10.5923/j.nn.20150501.01.

[15] S. R. Brintha and M. Ajitha, "Synthesis and characterization of ZnO nanoparticles via aqueous solution, sol-gel and hydrothermal methods," *IOSR J. Appl. Chem.*, vol. 8, no. 11, pp. 66–72, 2015, doi: 10.9790/5736-081116672.

[16] M. Parashar, V. K. Shukla, and R. Singh, "Metal oxides nanoparticles via sol–gel method: a review on synthesis, characterization and applications," *J. Mater. Sci. Mater. Electron.*, vol. 31, no. 5, pp. 3729–3749, 2020, doi: 10.1007/s10854-020-02994-8.

[17] K. Hayat, M. A. Gondal, M. M. Khaled, S. Ahmed, and A. M. Shemsi, "Nano ZnO synthesis by modified sol gel method and its application in heterogeneous photocatalytic removal of phenol from water," *Appl. Catal. A Gen.*, vol. 393, no. 1–2, pp. 122–129, 2011, doi: 10.1016/j.apcata.2010.11.032.

[18] S. Anandhi, A. Sagaya Amala Immanuel, V. Ramkumar, and C. Sudhakar, "Effect of solvent on ZnO nanoparticles by simple sol-gel method," *Mater. Today Proc.*, no. xxxx, 2023, doi: 10.1016/j.matpr.2023.06.232.

[19] Z. Wang, H. Li, F. Tang, J. Ma, and X. Zhou, "A Facile Approach for the Preparation of Nano-size Zinc Oxide in Water/Glycerol with Extremely Concentrated Zinc Sources," *Nanoscale Res. Lett.*, vol. 13, pp. 1–9, 2018, doi: 10.1186/s11671-018-2616-0.

[20] B. W. Chieng and Y. Y. Loo, "Synthesis of ZnO nanoparticles by modified polyol method," *Mater. Lett.*, vol. 73, pp. 78–82, 2012, doi: 10.1016/j.matlet.2012.01.004.

[21] A. S. Lanje, S. J. Sharma, R. S. Ningthoujam, J. S. Ahn, and R. B. Pode, "Low temperature dielectric studies of zinc oxide (ZnO) nanoparticles prepared by precipitation method," *Adv. Powder Technol.*, vol. 24, no. 1, pp. 331–335, 2013, doi: 10.1016/j.apt.2012.08.005.

[22] H. Li *et al.*, "Precursor-controlled synthesis of different ZnO nanostructures by the hydrothermal method," *Phys. Status Solidi Appl. Mater. Sci.*, vol. 211, no. 3, pp. 595–600, 2014, doi: 10.1002/pssa.201330037.

[23] R. Hong, T. Pan, J. Qian, and H. Li, "Synthesis and surface modification of ZnO nanoparticles," *Chem. Eng. J.*, vol. 119, no. 2–3, pp. 71–81, 2006, doi: 10.1016/j.cej.2006.03.003.

[24] C. Feldmann, "Polyol-mediated synthesis of nanoscale functional materials," *Solid State Sci.*, vol. 7, no. 7, pp. 868–873, 2005, doi: 10.1016/j.solidstatesciences.2005.01.018.

[25] I. Trenque, S. Mornet, E. Duguet, and M. Gaudon, "New insights into crystallite size and cell parameters correlation for ZnO nanoparticles obtained from polyol-mediated synthesis," *Inorg. Chem.*, vol. 52, no. 21, pp. 12811–12817, 2013, doi: 10.1021/ic402152f.

[26] A. Mezni *et al.*, "Facile synthesis of ZnO nanocrystals in polyol," *Mater. Lett.*, vol. 86, pp. 153–156, 2012, doi: 10.1016/j.matlet.2012.07.054.

[27] D. Visinescu *et al.*, "Additive-free 1,4-butanediol mediated synthesis: A suitable route to obtain nanostructured, mesoporous spherical zinc oxide materials with multifunctional properties," *RSC Adv.*, vol. 5, no. 121, pp. 99976–99989, 2015, doi: 10.1039/c5ra20224h.

[28] T. D. Canh, N. V. Tuyen, and N. N. Long, "Influence of solvents on the growth of zinc oxide nanoparticles fabricated by microwave irradiation," *VNU J. Sci. Math. - Phys.*, vol. 25, pp. 71–76, 2009.

[29] V. A and S. R. K, "Effect of Solvents on Particle Structure, Morphology and Optical Properties of Zinc Oxide Nano particles," *Int. J. Adv. Mater. Sci. Eng.*, vol. 4, no. 2, pp. 1–8, 2015, doi: 10.14810/ijamse.2015.4201.

[30] Z. Y. Shnain *et al.*, "The Effect of Solvent-Modification on the Physicochemical Properties of

ZnO Nanoparticles Synthesized by Sol-Gel Method," *Bull. Chem. React. Eng. Catal.*, vol. 17, no. 1, pp. 46–52, 2022, doi: 10.9767/bcrec.17.1.12345.46-52.

[31] H. K. Bùi, "Volume Synthesis By Sol-Gel Method And Characterization Of Zno Nanoparticles," vol. 1, no. 1, pp. 2–5, 2019.

[32] D. Bokov *et al.*, "Nanomaterial by Sol-Gel Method: Synthesis and Application," *Adv. Mater. Sci. Eng.*, vol. 2021, 2021, doi: 10.1155/2021/5102014.

[33] P. R. Shukla, S. Wang, H. M. Ang, and M. O. Tadé, "Photocatalytic oxidation of phenolic compounds using zinc oxide and sulphate radicals under artificial solar light," *Sep. Purif. Technol.*, vol. 70, no. 3, pp. 338–344, 2010, doi: 10.1016/j.seppur.2009.10.018.

[34] K. R. S. Murthy, R. G K, and P. Binnal, "Zinc Oxide Nanostructured Material for Sensor Application," *J. Biotechnol. Bioeng.*, vol. 5, no. 1, pp. 25–29, 2021, doi: 10.22259/2637-5362.0501004.

[35] K. Tyagi, "Estimation of toxic effects of chemically and biologically synthesized silver nanoparticles on human gut microflora containing Bacillus subtilis," *J. Toxicol. Environ. Heal. Sci.*, vol. 5, no. 9, pp. 172–177, 2013, doi: 10.5897/jtehs2013.0271.

[36] A. G. Pippa, "Interdisciplinary Postgraduate Studies Program in Nanomedicine ZINC OXIDE NANOPARTICLES : DESIGN , DEVELOPMENT AND STABILITY STUDIES," no. April, pp. 2022–2023, 2024.

[37] A. M. Ismail, A. A. Menazea, H. A. Kabary, A. E. El-Sherbiny, and A. Samy, "The influence of calcination temperature on structural and antimicrobial characteristics of zinc oxide nanoparticles synthesized by Sol–Gel method," *J. Mol. Struct.*, vol. 1196, pp. 332–337, 2019, doi: 10.1016/j.molstruc.2019.06.084.

[38] A. Putta and J. V. Vastrad, "Green synthesis and characterization of zinc oxide nanoparticles," *J. Eco-friendly Agric.*, vol. 18, no. 1, pp. 37–42, 2023, doi: 10.5958/2582-2683.2023.00007.2.

[39] M. A. Ismail, K. K. Taha, A. Modwi, and L. Khezami, "ZnO nanoparticles: Surface and X-ray profile analysis," *J. Ovonic Res.*, vol. 14, no. 5, pp. 381–393, 2018.

[40] N. Yusoff, L. N. Ho, S. A. Ong, Y. S. Wong, W. Khalik, and M. F. Ridzwan, "Enhanced photodegradation of phenol by ZnO nanoparticles synthesized through sol-gel method," *Sains Malaysiana*, vol. 46, no. 12, pp. 2507–2514, 2017, doi: 10.17576/jsm-2017-4612-28.

[41] G. Singh and S. P. Singh, "Synthesis of zinc oxide by sol-gel method and to study it's structural properties," *AIP Conf. Proc.*, vol. 2220, no. May, 2020, doi: 10.1063/5.0001593.

[42] I. Prabha and S. Lathasree, "Photodegradation of phenol by zinc oxide, titania and zinc oxide-titania composites: Nanoparticle synthesis, characterization and comparative photocatalytic efficiencfile:///C:/Users/almajd/Desktop/2_5296446230820304520.pdfies," *Mater. Sci. Semicond. Process.*, vol. 26, no. 1, pp. 603–613, 2014, doi: 10.1016/j.mssp.2014.05.031.

[43] K. I. Hamad, J. Y. Liao, T. W. Smith, and Y. Xing, "Synthesis of Layered

LiMn1/3Ni1/3Co1/3O2 Oxides for Lithium-Ion Batteries using Biomass-Derived Glycerol as Solvent," *Energy Technol.*, vol. 6, no. 4, pp. 710–717, 2018, doi: 10.1002/ente.201700646.

[44] K. I. Hamad, J. I. Humadi, Y. S. Issa, S. A. Gheni, M. A. Ahmed, and A. A. Hassan, "Enhancement of activity and lifetime of nano-iron oxide catalyst for environmentally friendly catalytic phenol oxidation process," *Clean. Eng. Technol.*, vol. 11, no. August, p. 100570, 2022, doi: 10.1016/j.clet.2022.100570.

[45] H. Dewidar, S. A. Nosier, and A. H. El-Shazly, "Photocatalytic degradation of phenol solution using Zinc Oxide/UV," *J. Chem. Heal. Saf.*, vol. 25, no. 1, pp. 2–11, 2018, doi: 10.1016/j.jchas.2017.06.001.

[46] A. Gnanaprakasam, V. M. Sivakumar, and M. Thirumarimurugan, "Influencing Parameters in the Photocatalytic Degradation of Organic Effluent via Nanometal Oxide Catalyst: A Review," *Indian J. Mater. Sci.*, vol. 2015, pp. 1–16, 2015, doi: 10.1155/2015/601827.

[47] N. Assi, P. A. Azar, M. S. Tehrani, and S. W. Husain, "Studies on photocatalytic performance and photodegradation kinetics of zinc oxide nanoparticles prepared by microwave-assisted sol–gel technique using ethylene glycol," *J. Iran. Chem. Soc.*, vol. 13, no. 9, pp. 1593–1602, 2016, doi: 10.1007/s13738-016-0875-1.